Materials Chemistry and Physics 154 (2015) 38–43

Contents lists available at ScienceDirect

Materials Chemistry and Physics

journal homepage: www.elsevier.com/locate/matchemphys

A low temperature reduction of CCl_4 to solid and hollow carbon nanospheres using metallic sodium

Mohammad Choucair [a, *], Matthew R. Hill [b], John A. Stride [c, d]

[a] School of Chemistry, University of Sydney, Sydney 2006, Australia
[b] CSIRO Division of Materials Science and Engineering, Private Bag 33, Clayton South MDC, Victoria 3169, Australia
[c] School of Chemistry, University of New South Wales, Sydney 2052, Australia
[d] Bragg Institute, Australian Nuclear Science and Technology Organisation, Kirrawee 2232, Australia

HIGHLIGHTS

- Sodium-mediated reduction of carbon tetrachloride to spherical carbon.
- We present a low-temperature method to realize carbon nanospheres.
- Spherical carbon material synthesized had high BET surface area.
- Hollow and solid spheres form with concentric arrangement.
- We examined the structure of chemically synthesized carbon material.

ARTICLE INFO

Article history:
Received 9 September 2014
Received in revised form
15 December 2014
Accepted 13 January 2015
Available online 16 January 2015

Keywords:
Nanostructures
Interfaces
Fullerenes
Electron microscopy
Microporous materials

ABSTRACT

Carbon nanospheres are obtained by reacting metallic sodium at 100 °C with tetrachloromethane under a flow of N_2 gas at ambient pressure. The product consisted of both hollowed and solid carbon spheres, ranging between 20 and 300 nm in size and comprised of concentrically oriented, disordered graphitic fragments. The maximum surface area recorded for this nanostructured carbon is 830 m^2 g^{-1}. Morphological, structural, and chemical analysis of the product is carried out with HR-TEM, BET surface area, XPS, XRD, and Raman spectroscopy. The formation of the spherical shape of the carbon nanoparticles is discussed based on direct observations of the reaction at the interfacial phase boundary.

1. Introduction

Carbon nanospheres (CNSs) are of inherent interest due to their high level of chemical activity as a result of differing degrees of porosity, making them suitable as membrane materials suited to gas-adsorption or catalyst supports [1], and a residual graphitic character, which may of interest in composite materials [2], energy storage [3], and electrochemical applications [4]. CNSs are generally not produced as discrete entities, but rather as a conglomeration of spherical bodies, often forming alongside tubular or filamentous carbons [5]. A definitive classification of spherical carbons is not straightforward, however an initial distinction of the overall morphology of spheres can be whether they are solid or hollow. More specifically, CNSs have been classified according to three proposed categories: concentric, radial or randomly oriented carbon layers [6].

These three categories have been further divided into groups according to their size: the C_n family and graphitic onion-like carbon with diameters in the range 2–20 nm, less graphitic onion-like carbon with diameters in the range of 20–50 nm, less graphitic carbon spheres 50 nm^{-1} μm, and carbon beads with diameters from 1 to 10 μm [7]. The degree of graphitization of CNSs is commonly evaluated by means of X-ray diffraction (XRD), Raman spectroscopy, and transmission electron microscopy (TEM) [5,7].

* Corresponding author.
E-mail address: mohammad.choucair@sydney.edu.au (M. Choucair).

http://dx.doi.org/10.1016/j.matchemphys.2015.01.042
0254-0584/

A comprehensive review of CNS production has been reported elsewhere [5] with current research suggesting the growth of CNSs requires high temperatures, typically between 950 and 1100 °C. Typical CNSs synthesis methods employ chemical vapour deposition under a gas flow, both with or without metal catalysts [8,9]. It has been determined that substantial CNSs growth proceeds by pyrolytic mechanisms, and that catalysts play only a minor role by assisting carbon growth and the determination of some lattice structures [10]. Chemical reduction using autoclaves at various pressures, often with the addition of transition metal catalysts, have significantly lowered the temperature required for the formation of CNSs to as low as 80 °C [11–15] and have also led to a range of carbon nanostructures including crumpled sheets [16], rods [17], tubes [18–20], belts [21] and even small amounts of diamond [22,23].

However, under typical solvothermal and hydrothermal conditions where autoclaves are used, it is not possible to make any direct visual observations of the reaction in process. In addressing this challenge, we have found a way to safely react sodium and CCl_4 under open reaction conditions to directly observe the reduction to CNSs. In so doing, major factors previously proposed to govern CNS formation at interfacial phase boundaries were verified [6] at one of the lowest confirmed temperatures that has yielded CNSs under gas flow [5]. We performed the reaction using reinforced borosilicate glassware able to withstand high heat densities, at ambient pressures, and a flow of N_2 gas. The highly exothermic reduction reaction was video recorded and provided in Supporting Material S1.

Supplementary data related to this article can be found online at http://dx.doi.org/10.1016/j.matchemphys.2015.01.042.

2. Experimental

2.1. Sample preparation

Sodium metal (0.83 g) was added to a three neck round bottom flask, under a flow of nitrogen gas and stirred using a magnetic stirrer bar encased in glass. The contents were heated using a sand bath, and the CCl_4 (1.65 g) was added drop-wise using a syringe (5 mL, 20 G). The reaction product was quenched with propanol then ethanol, and the product collected and stirred in milliQ water (100 mL) for 30 min. The black solid was filtered, and stirred in ethanol (80 mL) and hydrochloric acid (2 M, 20 mL) for 30 min. The product was dried under vacuum at 120 °C for 24 h. WARNING: Mixtures of sodium and CCl_4 are exceedingly dangerous. After standing for a short time, the reaction products are highly explosive [24].

2.2. Characterization

Transmission electron microscopy (TEM) was performed using a Philips CM200 operated at 200 kV. Powder X-ray diffraction (PXRD) data was collected over 10–60° 2θ range on a PANalytical X'Pert Pro diffractometer using Cu-K_α (λ = 1.5406 Å) radiation. Nitrogen adsorption isotherms were measured at 77 K on an Autosorb 1 over the range $2 \times 10^{-5} < P/P_o < 0.995$. The samples were degassed for 24 h prior to measurement. Pore size distribution was obtained using the Dubinin–Astakov method. Raman spectroscopy was conducted using a 514 nm green laser inVia Raman Spectrometer with 4 cm^{-1} resolution (10% laser power). X-ray photoelectron spectroscopy (XPS) was conducted on the as-prepared and washed carbon products using an ESCALAB 220i XL instrument and a monochromated Al K_α X-Ray source ($h\upsilon$ = 1486.6 eV) operated at 10 kV and 12 mA.

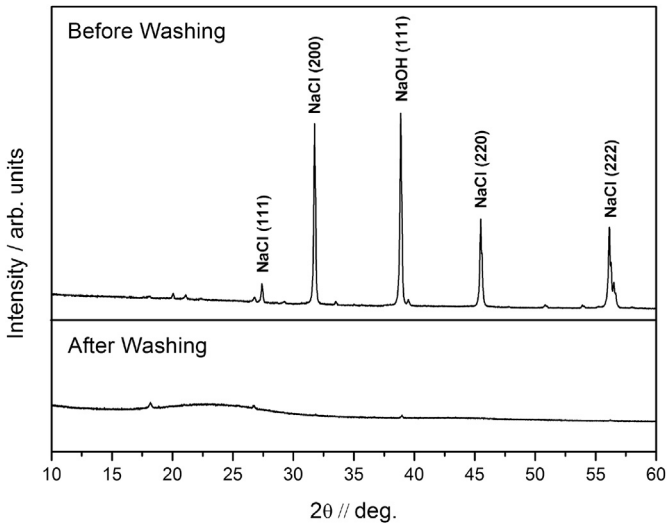

Fig. 1. Powder XRD of the reaction product before and after washing. After washing the sodium salts were effectively removed.

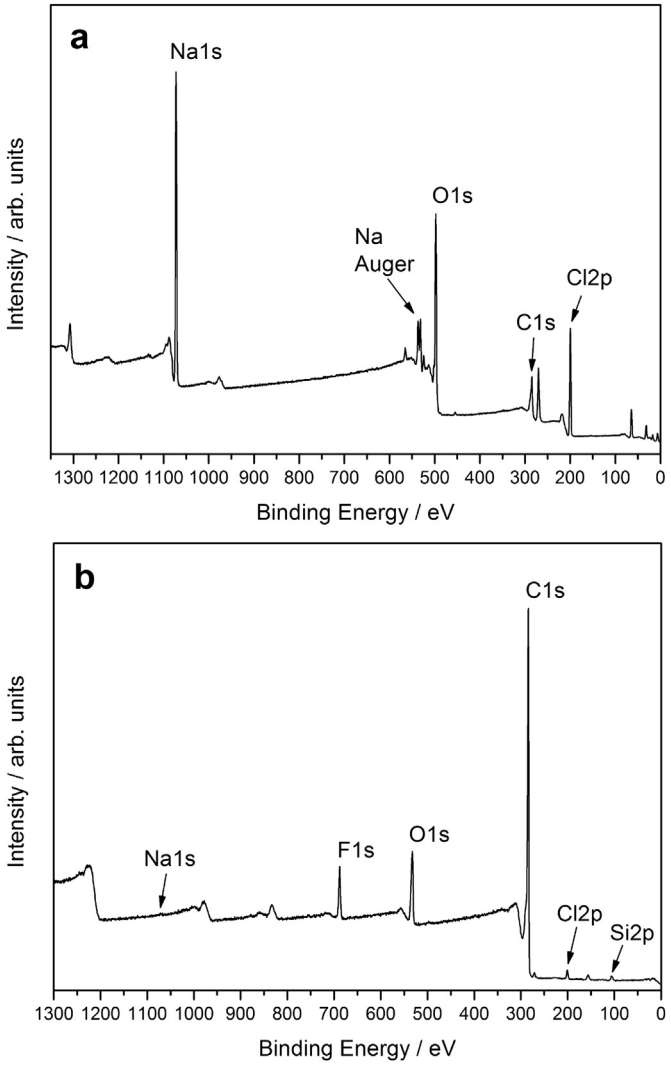

Fig. 2. XPS of (a) as-prepared sample and (b) washed sample.

3. Results & discussion

3.1. Results of CNS characterization

The as-prepared sample was initially studied using PXRD analysis, showing the presence of NaCl and NaOH, Fig. 1. However PXRD of the washed sample demonstrated the purification step was effective in removing most of the sodium salts and gave only broad diffraction peaks, consistent with scattering from amorphous carbon particles. The obtained interlayer spacing of the (002) graphitic plane, d_{002}, using the broad peak at $2\theta = 23.2°$, was *ca.* 0.383 nm. The d_{002} value obtained corresponds well with typical values reported for CNSs of 0.323–0.391 nm [5]. XPS quantified the amount of carbon in the final product to be 75.3 wt.% (atomic ratio C:O of 15:1), with remaining impurities including glass, Fig. 2.

Images taken by TEM show that carbon spheres of *ca.* 20–300 nm in diameter dominate the sample, Fig. 3, consistent with CNSs obtained in previously reported reactions [11,12,25]. Smaller individual hollow and solid spheres ranging from 20 to 50 nm in size are also evident. Spheres greater than 100 nm size generally appeared hollow. The larger hollowed spheres had a wall thickness of *ca.* 20 nm, made up of disordered graphitic layers.

Hollowed spheres larger than 100 nm had a distorted spherical shape, whilst upon closer inspection, the smaller (*ca.* 20 nm) solid spheres appeared to be concentric, with short-range graphitic fragments contributing to a disordered layering. The CNS formation extended over micron length scales as an agglomeration of spheres, tightly packed together and overlapping in the images, with some evidence of partial particle coalescence between smaller solid spheres similar to that observed in accreted spherical particles in soot [5].

The BET surface area of the carbon material increased from *ca.* 550 $m^2\ g^{-1}$ to *ca.* 830 $m^2\ g^{-1}$ with an increasing contribution made by the micropores present as the degas temperature was increased, Fig. 4.

The values of BET surface area obtained are amongst the highest reported for CNSs [5]. The benefits of degassing are large as the surface area value increases by *ca.* 50%. But this is limited to the early stages of the degas process (0–5 % weight loss, *i.e.* up to 300 °C). Beyond this point, the gain in BET surface area of the degassed material would be too small to compensate for the loss of material itself as carbon is removed from the structure during degassing as evidenced by thermal gravimetric analysis (Supporting information S2). As the carbon is removed the size of the pores also increases, which manifests as a steady increase of the micropore volume with degas temperature. The analysis suggests that the activation is acting in existing pores only and no new pores are being created in the process.

The Raman spectra of the CNSs is shown in Fig. 5 and shows a 'G band' centred at 1583 cm^{-1}, with a FWHM = 110 cm^{-1}, due to the in-plane stretching motion between pairs of sp^2 carbon atoms. This mode does not require the presence of sixfold rings, so it occurs at all sp^2 sites not only those in rings, and appears in the range 1500–1630 cm^{-1}. The presence of the 'D band' centred at 1381 cm^{-1}, with a FWHM = 269 cm^{-1}, is believed to be related to the number of ordered aromatic rings, and affected by the probability of finding a sixfold ring in a cluster. The intensity ratio of the D band to the G band value, commonly reported as I_D/I_G, was *ca.* 0.77,

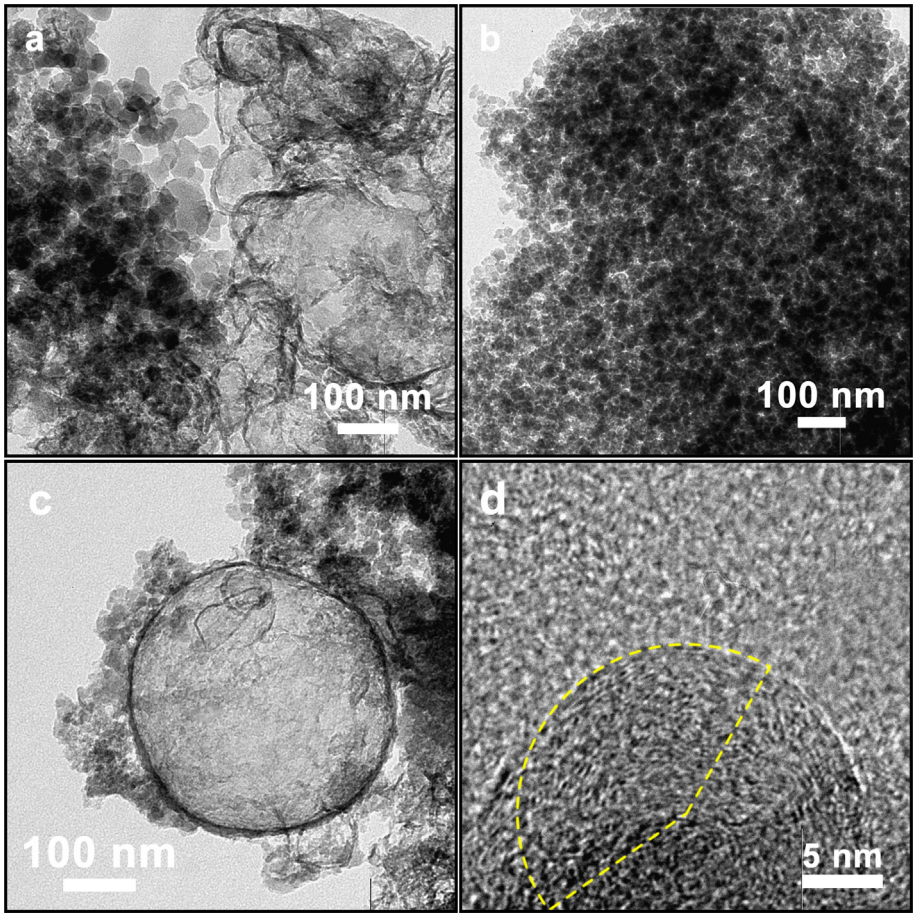

Fig. 3. TEM images of (a) a typical region of CNSs material (b) solid spheres (c) hollow sphere and (d) sphere with concentric arrangement of disordered graphite layers, the drawn sector is a guide for the eye.

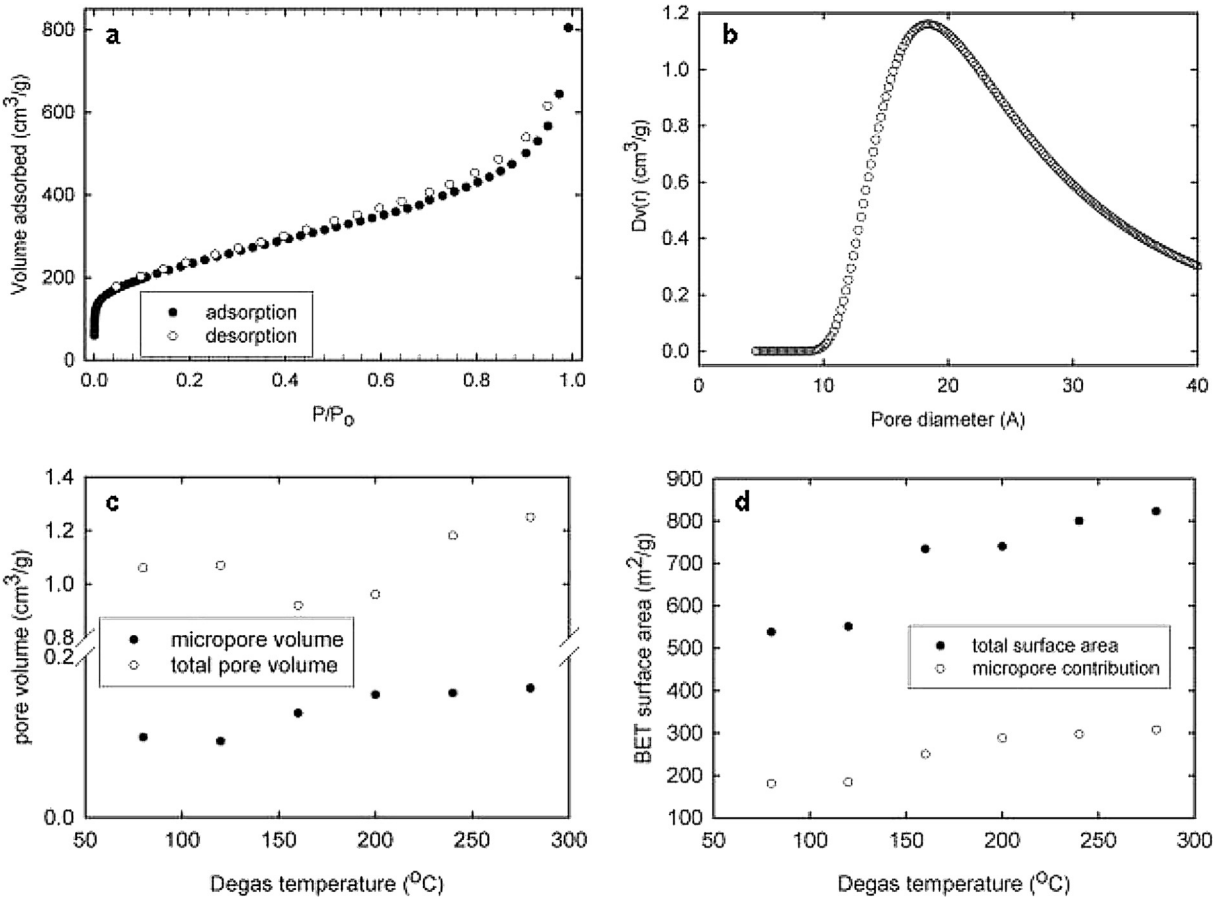

Fig. 4. (a) A typical 77 K N_2 isotherm of carbon material degassed at 280 °C. (b) Dubinin–Astakov plot for nitrogen sorption at 77 K. (c) Proportion of micropore volume to the total pore volume as a function of degas temperature. (d) Contribution of the micropore surface area to the overall measured BET surface area as a function of degas temperature.

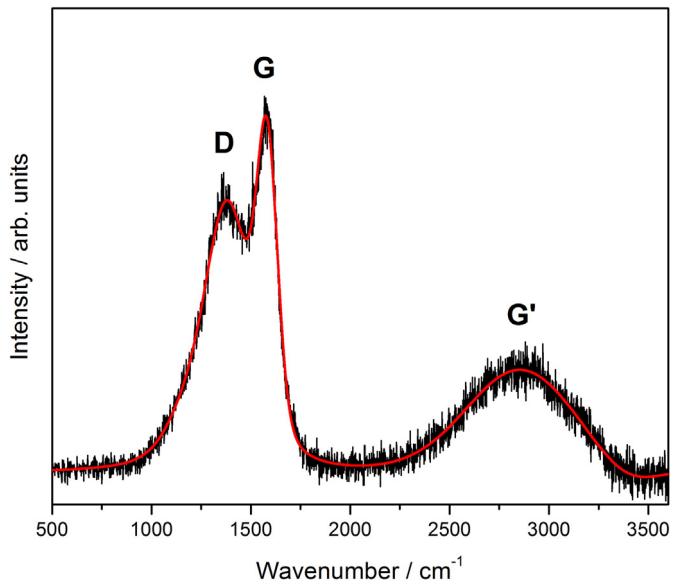

Fig. 5. Raman spectra of CNSs. Red line represents a Voigt peak fit to the data. (For interpretation of the references to colour in this figure legend, the reader is referred to the web version of this article.)

indicating a significant number of defect sites present within the CNSs [26]. This value compares well with reported I_D/I_G values for CNSs, which range between 0.8 and 1.2 [5]. The relative intensity and positions of the G and D bands have been interpreted to be due to sphere shell curvature coupled with the presence of defects and disorder in the short range graphitic fragments [27]. This is directly verified with TEM (Fig. 3). The identification of bands associated with other phases, which may also be present in smaller quantities (*e.g.* diamond), was not possible due to the background of the Raman spectrum contributions of disordered carbon.

3.2. Discussion of CNS formation

Liquid sodium effectively presents a fresh reactive surface to reagents that is continually reconstructed, fostering the reaction. This facet was confirmed by repeating the experiment below the melting point of sodium, for which no reaction was observed, and contact with the hot solid sodium surface simply caused the liquid CCl_4 to vaporize. The carbon material containing CNSs was directly observed to form with the $solid_{carbon}/liquid_{sodium}$ and $liquid_{sodium}/gas_{CCl4}$ interface with regions of non-homogenous energy dissipation (Supporting Information S1 video). Our current observations support several mechanistic elucidations which have been proposed regarding the formation of spherical carbon bodies [6,28–31] that highlight the interfacial energy as the major governing factor in determining the critical radius of a nucleated carbon sphere and the nano-texture of spherical carbon bodies at the stage of their formation.

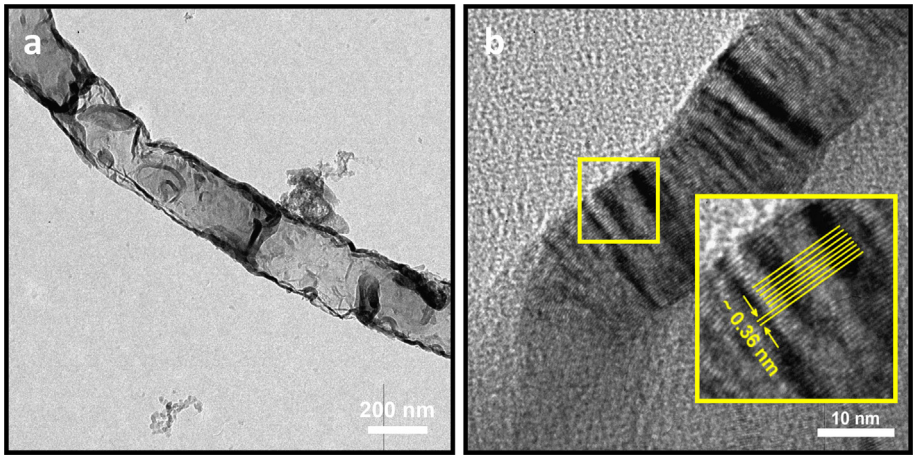

Fig. 6. (a) TEM image showing isolated crumpled graphitic sheets. (b) region at the edge of crumpled sheets showing *ca.* 50 layers with inter-layer spacing *ca.* 0.36 nm, more clearly magnified in the inset of the highlighted region indicated by the square. (For interpretation of the references to colour in this figure legend, the reader is referred to the web version of this article.)

As the interfacial energy is related strongly to the difference in surface energies between the two phases in contact at the interface, when the interfacial energy between these phases is reasonably large (*e.g.* between liquid/gas, solid/liquid, solid/gas), the concentric alignment of the basal planes of graphitic fragments to the surroundings acts to minimise the particle surface energy [6], which is consistent with the extensive formation of various size concentric CNSs in the present prepared material. Similarly, this mechanism has been attributed to the formation of fluid cokes by the decomposition of oils on a carbon surface where the solid/liquid and liquid/gas interface exists [6].

However, the mechanisms currently outlined are only reasonable when there is a strong interaction between the CNSs and their surroundings during formation. If the interfacial energy is insufficient to segregate and spherically arrange the graphitic fragments, the preferential orientation would then be along a graphitic reference plane *e.g.* yielding crumpled graphite, which is what Kuang et al. [16] primarily observe when employing solvothermal conditions to reduce CCl_4 with potassium. Crumpled graphitic structures *are* observed in our CNSs sample, although as discrete isolated bodies in extremely small number relative to the CNSs (Fig. 6), indicating that the current experimental conditions are ideal for facilitating the strong interaction of CNSs with their surroundings.

The strong interaction between the CNSs and the liquid$_{sodium}$/gas$_{CCl4}$ interface during formation is maintained by an excess of sodium as the CCl_4 is dosed into the reaction environment. The carbon formed at the reaction interface does not completely passivate the reactive sodium surface. The reaction proceeds with at least one interface, that of molten sodium, preserved. We observe convection currents at the molten sodium surface causing the surface to continually reconstruct. Variations in the difference in interfacial energy may occur as the CCl_4 is heated and undergoes transformation from liquid to gas upon contact with the sodium. To a first approximation, this results in the formation of different types of nested spheres (radial, concentric), and the curvature (or irregularity) associated with the reaction interface may give rise to non-uniform pressure fields (from mechanical strains, surface tension etc.) resulting in spheres of various sizes [32].

4. Conclusions

Spherical carbon material can be obtained by a one-step chemical reaction at temperatures as low as 100 °C under ambient pressure of N_2 using sodium to reduce CCl_4 without the use of transition metal catalysts. The reaction only proceeds at temperatures at or above the melting point of sodium: a transition from the solid to the liquid state allows the reaction to proceed with the exposure of a clean reaction surface. The results clearly highlight the importance of the reaction interface for the formation of spherical carbon bodies. The carbon material obtained had an exceptional BET surface area typical of porous and spherical carbon [5,33] suitable for consideration in future gas sorption and electrochemical applications.

Acknowledgements

M.C. acknowledges financial support from the University of Sydney.

Appendix A. Supplementary data

Supplementary data related to this article can be found at http://dx.doi.org/10.1016/j.matchemphys.2015.01.042.

References

[1] Z.C. Kang, Z.L. Wang, Chemical activities of graphitic carbon spheres, J. Mol. Catal. A Chem. 118 (1997) 215–222.
[2] Z.C. Kang, Z.L. Wang, On accretion of nanosize carbon spheres, J. Phys. Chem. 100 (1996) 5163–5165.
[3] L. Zubizarreta, J.A. Menéndez, J.J. Pis, A. Arenillas, Improving hydrogen storage in Ni-doped carbon nanospheres, Int. J. Hydrog. Energy 34 (2009) 3070–3076.
[4] P. Serp, R. Feurer, Y. Kihn, P. Kalck, J.L. Faria, J.L. Figueiredo, Novel carbon supported material: highly dispersed platinum particles on carbon nanospheres, J. Mater. Chem. 11 (2001) 1980–1981.
[5] A. Nieto-Marquez, R. Romero, A. Romero, J.L. Valverde, Carbon nanospheres: synthesis, physicochemical properties and applications, J. Mater. Chem. 21 (2011) 1664–1672.
[6] M. Inagaki, Discussion of the formation of nanometric texture in spherical carbon bodies, Carbon 35 (1997) 711–713.
[7] P. Serp, R. Feurer, P. Kalck, Y. Kihn, J.L. Faria, J.L. Figueiredo, A chemical vapour deposition process for the production of carbon nanospheres, Carbon 39 (2001) 621–626.
[8] X.-Y. Liu, B.-C. Huang, N.J. Coville, The Fe(CO)5 catalyzed pyrolysis of pentane: carbon nanotube and carbon nanoball formation, Carbon 40 (2002) 2791–2799.
[9] P. Wang, J. Wei, B. Huang, X. Qin, S. Yao, Q. Zhang, Z. Wang, G. Xu, X. Jing, Synthesis and characterization of carbon spheres prepared by chemical vapour deposition, Mater. Lett. 61 (2007) 4854–4856.
[10] A. Nieto-Márquez, J.C. Lazo, A. Romero, J.L. Valverde, Growth of nitrogen-doped filamentous and spherical carbon over unsupported and Y zeolite supported nickel and cobalt catalysts, Chem. Eng. J. 144 (2008) 518–530.
[11] G. Hu, D. Ma, M. Cheng, L. Liu, X. Bao, Direct synthesis of uniform hollow carbon spheres by a self-assembly template approach, Chem. Commun. (2002) 1948–1949.

[12] Y. Xiong, Y. Xie, Z. Li, C. Wub, R. Zhang, A novel approach to carbon hollow spheres and vessels from CCl4 at low temperatures, Chem. Commun. (2003) 904–905.
[13] X. Sun, Y. Li, Hollow carbonaceous capsules from glucose solution, J. Colloid Interface Sci. 291 (2005) 7–12.
[14] J. Xiao, M. Yao, K. Zhu, D. Zhang, S. Zhao, S. Lu, B. Liu, W. Cui, B. Liu, Facile synthesis of hydrogenated carbon nanospheres with a graphite-like ordered carbon structure, Nanoscale 5 (2013) 11306–11312.
[15] T.K. Ellis, C. Paras, M.R. Hill, J.A. Stride, Simple metal-catalyst-free production of carbon nanostructures, Aust. J. Chem. 66 (2013) 1435–1439.
[16] Q. Kuang, S.Y. Xie, Z.Y. Jiang, X.H. Zhang, Z.X. Xie, R. Huang, B.L.S. Zheng, Low temperature solvothermal synthesis of crumpled carbon nanosheets, Carbon 42 (2004) 1737–1741.
[17] X. Wang, J. Lu, Y. Xie, G. Du, Q. Guo, S. Zhang, A novel route to multiwalled carbon nanotubes and carbon nanorods at low temperature, J. Phys. Chem. B 106 (2002) 933–937.
[18] Y. Jiang, Y. Wu, S. Zhang, C. Xu, W. Yu, Y. Xie, Y. Qian, A catalytic-assembly solvothermal route to multiwall carbon nanotubes at a moderate temperature, J. Am. Chem. Soc. 122 (2000) 12383–12384.
[19] J. Liu, M. Shao, X. Chen, W. Yu, X. Liu, Y. Qian, Large-scale synthesis of carbon nanotubes by an ethanol thermal reduction process, J. Am. Chem. Soc. 125 (2003) 8088–8089.
[20] W. Wang, S. Kunwar, J.Y. Huang, D.Z. Wang, Z.F. Ren, Low temperature solvothermal synthesis of multiwall carbon nanotubes, Nanotechnology 16 (2005) 21–23.
[21] J. Liu, M. Shao, Q. Tang, S. Zhang, Y. Qian, Synthesis of carbon nanotubes and nanobelts through a medial-reduction method, J. Phys. Chem. B 107 (2003) 6329–6332.
[22] Y. Li, Y. Qian, H. Liao, Y. Ding, L. Yang, C. Xu, F. Li, G. Zhou, A reduction-pyrolysis-catalysis synthesis of diamond, Science 281 (1998) 246–247.
[23] Z. Lou, Q. Chen, W. Wang, Y. Qian, Y. Zhang, Growth of large diamond crystals by reduction of magnesium carbonate with metallic sodium, Angew. Chem. 115 (2003) 4639–4641.
[24] P. Urben, Bretherick's Handbook of Reactive Chemical Hazards, 2-vol. Set, Academic Press, 2006.
[25] D. Harbec, J.L. Meunier, L. Guo, G. . R., N.E. Mallah, Carbon nanotubes from the dissociation of C_2Cl_4 using a dc thermal plasma torch, J. Phys. D Appl. Phys. 37 (2004) 2121–2126.
[26] A.C. Ferrari, J. Robertson, Interpretation of Raman spectra of disordered and amorphous carbon, Phys. Rev. B 61 (2000) 14095–14107.
[27] E.D. Obraztsova, M. Fujii, S. Hayashi, V.L. Kuznetsov, Y.V. Butenko, A.L. Chuvilin, Raman identification of onion-like carbon, Carbon 36 (1998) 821–826.
[28] A. Nieto-Márquez, J.L. Valverde, M.A. Keane, Selective low temperature synthesis of carbon nanospheres via the catalytic decomposition of trichloroethylene, Appl. Catal. A General 352 (2009) 159–170.
[29] V.G. Pol, M. Motiei, A. Gedanken, J. Calderon-Moreno, M. Yoshimura, Carbon spherules: synthesis, properties and mechanistic elucidation, Carbon 42 (2004) 111–116.
[30] D. Ugarte, Formation mechanism of quasi-spherical carbon particles induced by electron bombardment, Chem. Phys. Lett. 207 (1993) 473–479.
[31] M. Choucair, J.A. Stride, The gram-scale synthesis of carbon onions,, Carbon 50 (2012) 1109–1115.
[32] A.W. Adamson, A.P. Gast, Physical Chemistry of Surfaces, sixth ed., Wiley-Interscience, New York, 1997.
[33] J. Jiang, Q. Gao, Z. Zheng, K. Xia, J. Hu, Enhanced room temperature hydrogen storage capacity of hollow nitrogen-containing carbon spheres, Int. J. Hydrog. Energy 35 (2010) 210–216.